



1 **Spring snow albedo feedback over Northern Eurasia:**

2 **Comparing in-situ measurements with reanalysis products**

3 Martin Wegmann<sup>1</sup>, Emanuel Dutra<sup>2</sup>, Hans-Werner Jacobi<sup>1</sup> and Olga Zolina<sup>1,3</sup>

4 <sup>1</sup>*Institute for Geosciences and Environmental Research (IGE), Univ. Grenoble Alpes,*  
5 *CNRS, IRD, Grenoble INP\*, Grenoble, France*

6 *\* Institute of Engineering Univ. Grenoble Alpes*

7 <sup>2</sup>*Instituto Dom Luiz, Faculdade de Ciências, Universidade de Lisboa, Lisbon,*  
8 *Portugal*

9 <sup>3</sup>*P.P. Shirshov Institute of Oceanology, Moscow, Russia*

10

11

12

13

14

15

16

17

18

19

20

21

22

23



24 ABSTRACT

25 This study uses daily observations and modern reanalyses in order to evaluate  
26 reanalysis products over Northern Eurasia regarding the spring snow albedo feedback  
27 (SAF) during the period from 2000 to 2013. We used the state of the art reanalyses  
28 ERA-Interim land and the Modern-Era Retrospective Analysis for Research and  
29 Applications Version 2 (MERRA2) as well as an experimental setup of ERA-Interim  
30 land with prescribed short grass as land cover to enhance the comparability with the  
31 station data. While snow depth statistics derived from daily station data are well  
32 reproduced in all three reanalyses, the day-to-day variability of the albedo is notably  
33 higher at stations compared to any reanalysis product. The ERA-Interim grass setup  
34 shows an improved performance in representing albedo variability and generates  
35 comparable estimates for the snow albedo in spring. We find that modern reanalyses  
36 show a physically consistent representation of SAF, with realistic spatial patterns and  
37 area-averaged sensitivity estimates. However, station-based SAF values are  
38 significantly higher than in the reanalyses, which is mostly driven by the stronger  
39 contrast between snow and snow-free albedo. Switching to grass-only vegetation in  
40 ERA-Interim land increases the SAF values up to the level of station-based estimates.  
41 We found no significant trend in the examined 14-year timeseries of SAF, but inter-  
42 annual changes of about  $0.5\% K^{-1}$  in both station-based and reanalysis estimates were  
43 derived. This inter-annual variability is primarily dominated by the variability in the  
44 snow melt sensitivity, which is correctly captured in reanalysis products. Although  
45 modern reanalyses perform well for snow variables, efforts should be made to  
46 improve the representation of dynamic albedo changes.

47

48

49

50

51

52

53



## 54 1. Introduction

55 Global warming is enhanced at high northern latitudes, where the Arctic near-surface  
56 air temperature has risen at twice the rate of the global average in recent decades – a  
57 feature called Arctic amplification (**Serreze and Barry 2011**). Climate model  
58 experiments for the 21st and 22nd centuries show that the Arctic warming will  
59 continue and intensify under all emission scenarios (**Collins et al. 2013**). Arctic  
60 amplification of the global warming signal results from several processes interacting  
61 with each other such as the albedo feedback due to a reduction in snow and ice cover,  
62 enhanced poleward atmospheric and oceanic heat transport, and changes in humidity  
63 (**Serreze and Barry 2011**).

64  
65 Being one of the critical factors of the Arctic amplification, the surface albedo  
66 feedback implies that the additional amount of reflected shortwave radiation at the top  
67 of the atmosphere decreases with decreasing surface albedo whereas near-surface air  
68 temperature increases with decreasing surface albedo (**Thackeray and Fletcher**  
69 **2016**). It is considered to be a positive feedback in the sense that an initial warming  
70 leads to a warming strengthening over time quantified through the change in surface  
71 albedo per unit change of temperature (**Robock 1983, Cess et al. 1991, Qu and Hall**  
72 **2007**). Snow can cause such a feedback since a snow-free surface absorbs more  
73 shortwave radiation and converts the energy to longwave radiation and convection,  
74 which warm the lower layers of the troposphere (**Curry et al. 1996**). This snow  
75 albedo feedback (SAF) and its impact on climate have been studied for several  
76 decades (**Wexler et al. 1953, Budyko 1969, Schneider and Dickinson 1974, Lian**  
77 **and Cess 1977**). It got further attention in the wake of anthropogenic global warming  
78 accompanied by the reduction of snow and ice cover over the Northern Hemisphere  
79 (**Bony et al. 2006, Qu and Hall 2007, Fernandes et al. 2009, Flanner et al. 2011,**  
80 **Qu & Hall 2014, Fletcher et al. 2015, Thackeray and Fletcher 2016**).

81  
82 During 1979–2011, the Arctic snow cover extent in June decreased at a rate of -21%  
83 per decade (**Derksen and Brown 2012**). Climate model projections for the end of the  
84 21st century show an even more reduced Arctic cryosphere and, thus, the SAF will  
85 continue to modulate Arctic warming (**Brutel-Vuilmet et al. 2013**). The SAF is  
86 especially effective over the Northern Hemisphere (NH) since most of the NH is



87 covered by snow during boreal wintertime (**Groisman et al. 1994**). **Hall (2004)** found  
88 that 50% of the total NH SAF caused by global warming occurs during spring, while  
89 **Qu and Hall (2014)** estimated that the SAF variability accounts for 40-50% of the  
90 spread in the warming signal over the continents of the NH.

91

92

93 Several studies investigated spring NH SAF based on satellite, reanalysis and model  
94 datasets (**Fernandes et al. 2009**, **Fletcher et al. 2012**, **Qu and Hall 2014**, **Fletcher et**  
95 **al. 2015**). Satellite-based estimates of SAF vary within  $\pm 10\%$  depending on the  
96 analysed data set. **Hall et al. (2008)** used the International Satellite Cloud  
97 Climatology Project (ISCCP) data (**Schiffer and Rossow 1983**) to calculate an SAF  
98 strength of  $-1.13\% \text{ K}^{-1}$ , whereas **Fernandes et al. (2009)** using Advanced Very High  
99 Resolution Radiometer (AVHRR) data (**Justice et al. 1985**) found a slightly weaker  
100 SAF of  $-0.93\% \text{ K}^{-1}$ . **Qu and Hall (2014)** determined the SAF using Moderate  
101 Resolution Imaging Spectroradiometer (MODIS) data (**Hall et al. 2002**) and found a  
102 value of  $-0.87\% \text{ K}^{-1}$  for springtime. Considering different spatial and temporal  
103 domains as well as the variety of methods applied, the SAF estimates around  $-1\% \text{ K}^{-1}$   
104 from satellite data can be considered as quantitatively consistent.

105

106 Model- and reanalysis-based estimates are somewhat higher compared to those  
107 derived from satellite data. **Fletcher et al. (2015)** investigated CMIP3 and CMIP5  
108 ensembles to estimate the SAF for an assortment of Global Climate Models (GCMs).  
109 From a large set of SAF estimates for individual models, they found an ensemble  
110 mean of  $-1.2\% \text{ K}^{-1}$  which is in fair agreement with MODIS values, but is higher  
111 compared to ISCCP- and AVHRR-based estimates. Within this comparison **Fletcher**  
112 **et al. (2015)** also investigated SAF computations based on ERA-Interim (**Dee et al.**  
113 **2011**), Modern-Era Retrospective Analysis for Research and Applications (MERRA)  
114 (**Rienecker et al. 2011**) and NCEP-2 (**Kanamitsu et al. 2002**) reanalyses, thus,  
115 providing the most up to date assessment of SAF in reanalysis datasets. While  
116 MERRA data resulted in a slightly weaker SAF of  $-1.17\% \text{ K}^{-1}$  compared to ERA-  
117 Interim ( $-1.23\% \text{ K}^{-1}$ ), both reanalyses show similar SAF values compared to MODIS.

118



119 Although satellite products cover large parts of the NH, they exhibit low temporal  
120 resolution and significant uncertainties for high solar zenith angles as well as complex  
121 terrains (eg. **Wang et al. 2014**). **Thackeray and Fletcher (2016)** compared  
122 CMIP3/CMIP5 model families and found that the models represent the SAF process  
123 rather accurately. However, there are still inherent biases likely related to the use of  
124 outdated parameterizations. In this respect the use of in-situ observations would  
125 provide an opportunity for evaluating SAF estimates in different gridded datasets and  
126 especially among reanalyses. However, estimating SAF in the Arctic using in-situ  
127 data is challenging, mostly because of the lack of reliable, relevant observations, both  
128 in the temporal and spatial domain. Furthermore, the lack of in-situ SAF estimates  
129 hampers the understanding of SAF in high latitude climates (**Graversen and Wang**  
130 **2009, Gravesen et al. 2014**).

131  
132 In this study we use a unique dataset of daily observations and modern reanalyses  
133 over Northern Eurasia in order (1) to evaluate reanalysis products with respect to  
134 radiation and snow properties and (2) to determine the SAF in spring between 2000–  
135 2013 based on in-situ measurements. We compare different land-reanalysis products  
136 with modified vegetation settings. Specific questions to be addressed in this study are  
137 the following: How well do the modern reanalyses reproduce snow and radiation  
138 features on a daily resolution? What are realistic estimates of the SAF from the station  
139 data over Northern Eurasia and how well do they compare to the gridded reanalyses  
140 data? What are the major characteristics of space-time variability of the SAF in  
141 station and reanalysis data?

142  
143 The paper is organized as follows. After describing the different datasets and the  
144 methods in sections 2 & 3, we evaluate the daily output for snow, radiation fluxes and  
145 temperature within these datasets in section 4.1. In section 4.2 we assess the results of  
146 the SAF computations and the differences between products including also an  
147 analysis of the spatial and temporal variability. Section 5 discusses the results and  
148 considers potential implications for future studies.

149

## 150 **2. Data**

### 151 **2.1 Reanalysis Data**



152 To investigate the SAF processes in reanalyses, we evaluated two products: the ERA-  
153 Interim-land (ERA-I-L, **Balsamo et al. 2015**) and Modern-Era Retrospective analysis  
154 for Research and Applications, Version 2 (MERRA2) (**Gelaro et al. 2017**). ERA-I-L  
155 is a land-surface only simulation driven by the near-surface meteorology and fluxes  
156 from the ERA-Interim atmospheric reanalyses (**Dee et al. 2011**). The land-surface  
157 model in ERA-I-L (HTESSEL) has several enhancements compared with the land-  
158 surface model used in ERA-Interim including the snowpack representation (**Dutra et**  
159 **al. 2010**). ERA-I-L considers the prognostic evolution of snow mass and density, and  
160 for exposed areas there is also a prognostic evolution of snow albedo. For shaded  
161 snow, i.e. snow under high vegetation, the albedo is considered constant and  
162 dependent on vegetation type (see **Dutra et al. 2010** for more details). Since the  
163 observations used in this study are local, and in the case of forest regions likely  
164 represent a clearcut in the forest, idealized simulations prescribing grassland  
165 everywhere were carried out with the ERA-I-L configuration (hereafter ERA-Interim  
166 land grass only (ERA-I-LG)). The main goal of this simulation is to evaluate the role  
167 of land cover when comparing point observations with gridded reanalysis and to  
168 evaluate pathways to improve reanalyses in representing albedo processes.

169 MERRA2 also includes a dedicated land module for surface variables. Furthermore, it  
170 applies an updated Goddard Earth Observing System (GEOS) model and analysis  
171 scheme and assimilates more observations than its predecessor MERRA (**Rienecker**  
172 **et al. 2011**). Finally, MERRA2 uses observation-based precipitation data to force its  
173 land-surface parameterizations, similar to what formerly was known as MERRA-land.  
174 Unlike ERA-I-L, MERRA2 consists of a full land-atmosphere reanalysis. Its  
175 incremental analysis update (IAU) scheme improves upon 3D-Var by dampening the  
176 analysis increment. In IAU, a correction is applied to the forecast model gradually,  
177 limiting precipitation spinup in particular.

178 For near-surface temperature we use 2m air temperature for both the reanalyses and  
179 observations. Moreover, we do not use albedo diagnosed by the reanalysis, but  
180 calculate it from the radiative flux components consistent with the observed albedo.  
181 For this purpose we use upward and downward shortwave radiation at the surface as  
182 diagnosed by ERA-Interim and MERRA2 as well as surface net and surface incoming  
183 radiation from the station observations. Snow depth is used as diagnosed by  
184 reanalyses and, if needed, converted to cm.



185 More information about general characteristics of reanalysis products in the Arctic  
186 can be found in **Lindsay et al. (2014)**, **Dufour et al. (2016)** and **Wegmann et al.**  
187 **(2017)**.

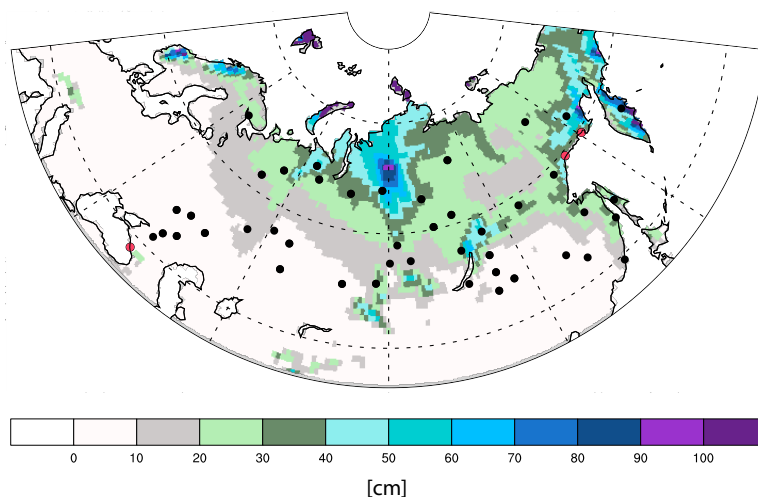
## 188 **2.2 Observational in-situ data**

189 To evaluate reanalysis performance, we used newly assembled in-situ radiation  
190 observations from Russian meteorological stations. This dataset includes 4-hourly  
191 Solar Radiation and Radiation Balance Data from the WMO World Radiation  
192 Network of the World Radiation Data Center (WRDC) at the Voeikov Main  
193 Geophysical Observatory, Saint Petersburg, Russia. The original WRDC data  
194 contains time series (1964–2015) from 65 locations. Of these, we selected 47  
195 stations for this study because they overlap with daily snow depth and 2m temperature  
196 observations (see Supplement Table 1). Of these 47 stations three were attributed by  
197 ERAI-L to ocean areas, so that the final dataset consists of 44 stations. Temperature  
198 and snow depth observations were taken from the All-Russian Research Institute of  
199 Hydrometeorological Information World Data Centre (RIHMI-WDC), Obninsk,  
200 Russia. A detailed description of this dataset is provided by **Bulygina et al. (2010)**.  
201 This dataset includes snow depth as well as snow cover over an area around  
202 meteorological stations. Snow cover information in this data set is not stored in  
203 percentages, but rather in a scale of integers from 0 to 10 (for example, 50% is  
204 assigned a value of 5, but so is 53%). This makes these data hardly applicable for  
205 precise SAF calculations. Snow depth information is measured in centimeters with the  
206 precision of 1 cm. This might lead to an underestimation of snow depth in case of  
207 shallow snow (between 0 and 1 cm). All variables (temperature, snow depth and snow  
208 cover, surface LW radiation budget and surface SW radiation, the sum of the surface  
209 short-wave and long-wave radiation budgets) were represented as daily time series for  
210 the period 2000–2013.

211 Figure 1 shows the location of the stations together with the climatological 2000–  
212 2013 MAMJ snow depth as computed by ERAI-L. The distribution of stations is quite  
213 heterogeneous, with very few stations located in Eastern Siberia and in the Far East.  
214 Moreover, some stations have prolonged periods of missing values; six stations have  
215 more than 50% missing values in the daily timeseries for MAMJ. For monthly means,  
216 the total number of missing values generally decreases from 2000 to 2013 (see



217 Supplementary Figure 1), However, data for the year 2009 are missing at 44 out of 47  
218 stations for the MAM period and for 3 stations also June values are missing.  
219 Nevertheless, spatial and temporal coverage of this data set is exceptional for the  
220 analysis of albedo in this region. It is also important to note that neither snow nor  
221 radiation from these stations were assimilated in the reanalysis datasets and, therefore,  
222 our inter-comparisons are completely independent.



223

224 **Figure 1: Station location and snowdepth [cm] for the 2000–2013 MAMJ average taken from ERAI-L.**  
225 **Red colored stations are excluded by the land-sea mask of ERAI-L.**

226

### 227 3. Methods

228 To evaluate the climatic variables needed for the SAF computation, we first compared  
229 daily values of snow depth, albedo and 2m temperature from the meteorological  
230 stations with those from the reanalyses. To co-locate observations with reanalyses, we  
231 extracted the information of the gridcell from the reanalysis, in which the station is  
232 located. We then derived long-term differences, performed a correlation analysis and  
233 also compared the variability among the datasets for the MAMJ period.





234 Since the SAF signals for the seasonal cycle and for the long-term climate change  
235 signal are highly correlated (Hall and Qu 2006), we focus here on the evaluation of  
236 the seasonal cycle. Snow cover is converted from snow depth following a logarithmic  
237 equation according to which 2.5 cm of snow depth was defined as equivalent to 100%  
238 snow cover (Fletcher et al. 2015). In most analyses, SAF is split into a snow cover  
239 component (SNC) and a temperature/metamorphosis component (TEM). SNC relates  
240 to the decrease of the albedo linked to the earlier melting of snow, which causes the  
241 exposition of the surface with a much reduced albedo. TEM concerns the reduction of  
242 snow albedo due to enhanced metamorphism and larger grain sizes at warmer  
243 temperatures. SAF is computed as sum of the two components, SNC and TEM,  
244 according to:

245

$$246 \quad \mathit{SNC} = (\overline{\alpha_{\mathit{snow}}} - \alpha_{\mathit{land}}) \Delta \mathit{S}_c / \Delta \mathit{T}_{2m} \quad (1)$$

247 and

$$248 \quad \mathit{TEM} = \overline{\mathit{S}_c} \Delta \alpha_{\mathit{snow}} / \Delta \mathit{T}_{2m} \quad (2)$$

249 where  $\alpha_{\mathit{snow}}$  is the snow-covered surface albedo,  $\alpha_{\mathit{land}}$  is the snow-free surface  
250 albedo,  $\mathit{S}_c$  is the snow cover fraction and  $\mathit{T}_{2m}$  is the 2 m temperature. The first term  
251 of (1) is also known as albedo contrast, whereas the second term will be referred to as  
252 snow melt sensitivity. In (1) and (2) deltas indicate month-to-month changes and the  
253 overbars indicate means over the two adjacent months. Note that  $\Delta \mathit{T}_{2m}$  does not  
254 represent a hemispheric mean but rather the difference at an individual location. It  
255 was found that the contribution of SNC and TEM to the overall SAF is between 60 to  
256 70% and 30 to 40 % for the NH (Fletcher et al. 2015).

257 Since daily data are available, we define  $\alpha_{\mathit{snow}}$  as the monthly mean over all daily  
258 estimates during the specific month when  $\mathit{S}_c = 100\%$ . Moreover, we define  $\alpha_{\mathit{land}}$   
259 as the mean over all daily estimates during MAMJ when  $\mathit{S}_c = 0\%$ . This allows for a  
260 more realistic estimation of  $\alpha_{\mathit{land}}$  than conventionally using summer (e.g. August)  
261 albedo.

## 262 4 Results

### 263 4.1 Daily data evaluation



264 Since 2m air temperature in reanalyses has been comprehensively evaluated in  
265 previous studies (eg. **Schubert et al. 2014**, **Lindsay et al. 2014**), We only perform a  
266 general comparative assessment of the daily values of albedo and snow depth involved  
267 in the SAF computations.

268 Figure 2 shows an overall comparison between station data and reanalyses in terms of  
269 correlations, differences and magnitude of variability quantified by the standard  
270 deviation for the albedo and snow depths. On a day-to-day basis MERRA2 and  
271 ERAI-L are underestimating average albedo values compared to observations by  
272 about 0.1 during MAMJ (Figure 2a). On the other hand, ERAI-LG shows a much  
273 smaller average deviation from the station data with differences close to zero.  
274 However, the overall range of the boxplot for ERAI-LG is similar to the other two  
275 reanalyses resulting in only slightly less absolute deviations from the observations.

276 For snow depth (Figure 2b), all three reanalysis datasets show an overestimation of  
277 daily values for MAMJ. Interestingly, ERAI-LG shows the largest deviations from  
278 observed values, although the grass represents better the conditions at the  
279 observational sites. This can be caused by biases in the observations due to  
280 surrounding higher vegetation creating a snowfall shadow or negative instrumental  
281 biases (**Rasmussen et al. 2012**). Moreover, positive biases in particular for  
282 precipitation can occur in reanalysis products (**Brun et al. 2013**).

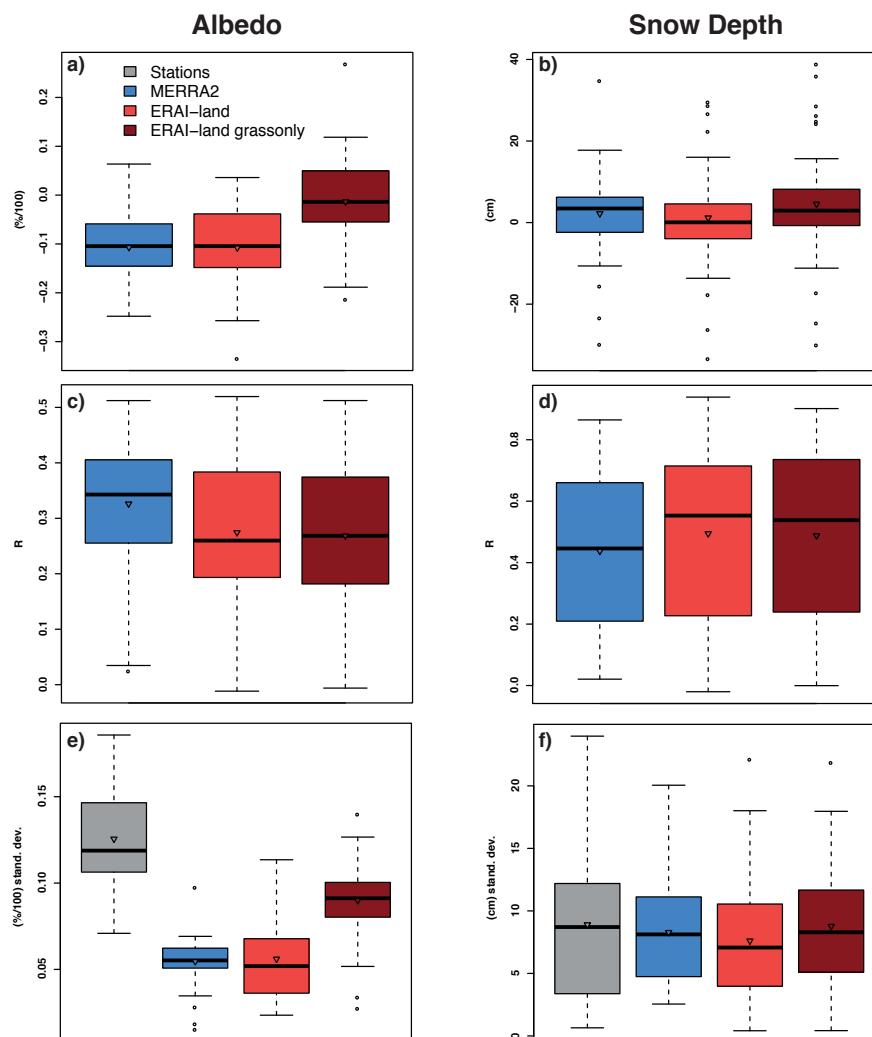
283 The analysis of daily correlations (Figure 2 c and d) demonstrates that the correlations  
284 for the albedo are generally low among all three experiments, whereas for some  
285 stations they can reach correlation coefficients higher than 0.8. Surprisingly, the  
286 correlations between MERRA2 and station data are the highest for albedo and the  
287 lowest for snow depth. The observed difference between MERRA2 and the ECMWF  
288 experiments regarding the correlation for albedo can likely be explained by the  
289 introduction of aerosols (and their respective deposition) in MERRA2. These findings  
290 suggest that further studies are needed to investigate the impact of aerosols on snow  
291 albedo representation. For snow depth, the correlation values are dominated by  
292 snowfall and melting events. Also in this case, the grass-only experiment shows no  
293 increased performance compared to the classic ERAI setup.

294 Considering the representation of day-to-day variability (Figure 2 e and f), all  
295 reanalyses severely underestimate the day-to-day variability of the albedo. MERRA2



296 and ERAI-L show similar means, but reach the overall station level only in specific  
297 grid cells. A clear improvement is observed in ERAI-LG, which shows the smallest  
298 deviation from station estimates. Nevertheless, all modern reanalyses fail to  
299 adequately reproduce daily variability in the observed albedo. On the other hand, for  
300 snow depth the agreement is very good. The means of all four products are around the  
301 values of 8 to 10 cm, with the grass-only experiment being the closest to the average  
302 station variability.

303 In summary, the boxplot analysis (Figures 2) reveals that there is a general  
304 improvement in agreement between stations and ERAI-L if vegetation is set to grass  
305 only. However, none of the reanalysis products can accurately reproduce day-to-day  
306 albedo variability. This is likely explained by the comparison of grid versus point  
307 observations, where small-scale variations are averaged out. Moreover, observed  
308 snow-free albedo depends on short-term changes linked to the vegetation and  
309 meteorology for example causing frost or modifying soil moisture.



310

311 **Figure 2: Boxplot analysis for daily albedo (a, c, e) and snow depth (b, d, f) estimates using data from**  
312 **44 locations over 2000–2013 MAMJ period. (a) and (b) Difference between station and reanalysis,**  
313 **(c) and (d) linear correlation between station and reanalysis, (e) and (f) standard deviation.**  
314 **Triangle indicates the mean value.**

315

316

317

318



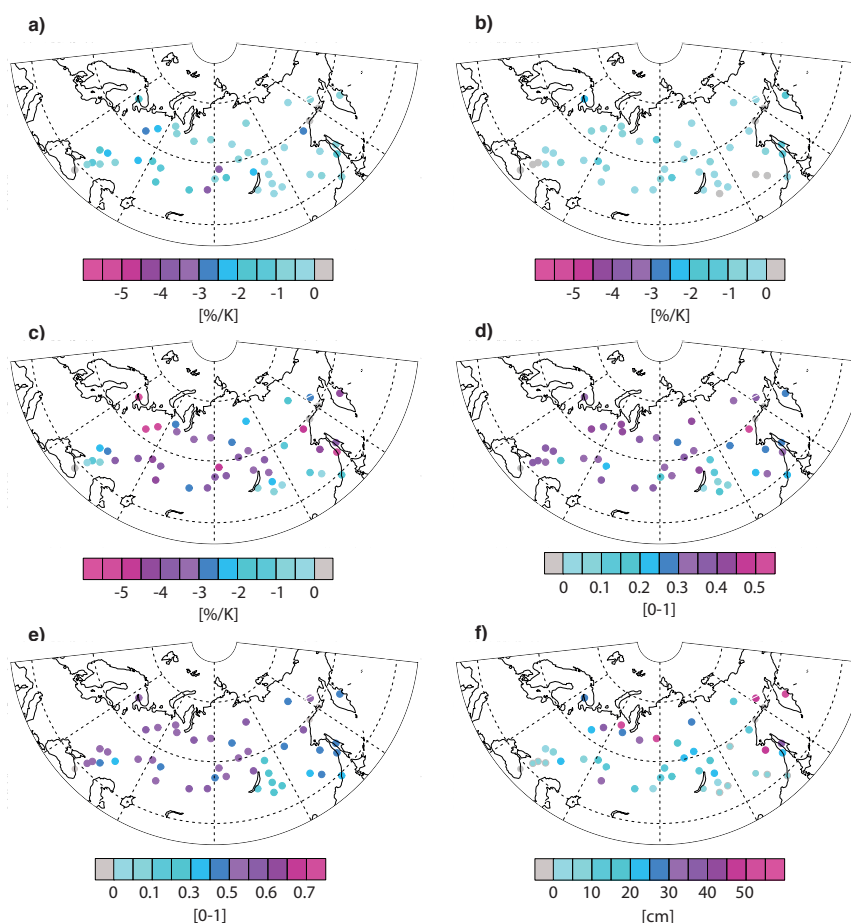
#### 319 **4.2 Analysis of feedback components**

320 To assess regional patterns of key SAF components, we show their spatial distribution  
321 over Russia as revealed by the observations in Figure 3 (See Supplement Figures 2-4  
322 for the respective distribution from the reanalyses data).

323 Strong SNC (Figure 3a) responses in the station data are observed in Southern  
324 European Russia and Western Siberia as well as over the Far East. The weaker  
325 responses are observed in Southern Eastern Siberia. TEM (Figure 3b) follows a  
326 similar distribution but is more homogeneously distributed with most negative values  
327 in Central Siberia and towards the Arctic coastline. Snow melt sensitivity (Figure 3c)  
328 is strongest in the mid-latitudinal and subpolar regions north of 50° N, such as  
329 Finland to the southeast, west and north of Lake Baikal and along the Pacific  
330 Coast. Here the temperatures react most strongly to seasonal snow melt. While there  
331 is a broad agreement between the stations and ERAI-LG in this region, stations show  
332 a somewhat stronger snow melt sensitivity (not shown). Snow melt sensitivity is a key  
333 factor for the SNC calculations and, thus, shapes the spatial variability of SNC.

334 The other key factor in the SNC calculations is the contrast in albedo between snow-  
335 covered and snow-free periods (Figure 3d). The observed albedo contrast is  
336 characterized by a relatively homogeneous pattern with somewhat smaller values in  
337 the southern regions, especially over Southern Eastern Siberia east of the Lake Baikal.  
338 In general, a north-south gradient is visible with similar patterns as in SNC. Mean  
339 albedo for the spring season (Figure 3e) shows that highest values are found closer to  
340 the Arctic coastline, in Central Siberia and towards the western border. Lower mean  
341 albedo values are mostly located east of Lake Baikal. This distribution is in general  
342 agreement with the reanalyses datasets, especially for the lower values in the south  
343 east.

344 Finally, since TEM follows closely the general MAMJ snow distribution, we show  
345 average snow depth in Figure 3f. A clear north-south gradient is visible with hotspots  
346 at the Pacific coast and towards the Barents-Kara sea. Moreover, snow depths from  
347 stations follow closely the ERA-L snowdepth distribution shown in Figure 1.



348

349 **Figure 3: Mean SAF components in the station for 2000–2013 MAMJ. a) SNC, b) TEM, c) snow melt**  
 350 **sensitivity, d) mean albedo contrast, e) mean albedo, f) snow depth.**

351

352 To analyse the differences between the datasets and to highlight the context of the  
 353 station data, Figure 4a shows the response for SAF computed for the entire period  
 354 2000-2013 and all 44 locations. Stations show much stronger SAF ( $-2.5\% \text{ K}^{-1}$ )  
 355 compared to MERRA ( $-1.6\% \text{ K}^{-1}$ ) and ERAI-L ( $-1.8\% \text{ K}^{-1}$ ). At the same time ERAI-  
 356 LG shows SAF estimate close to that derived from the station data ( $-2.8\% \text{ K}^{-1}$ ). Thus,  
 357 changing the vegetation to short grass adds about 1 K to the responses revealed by  
 358 classic reanalyses making the results close to observations.

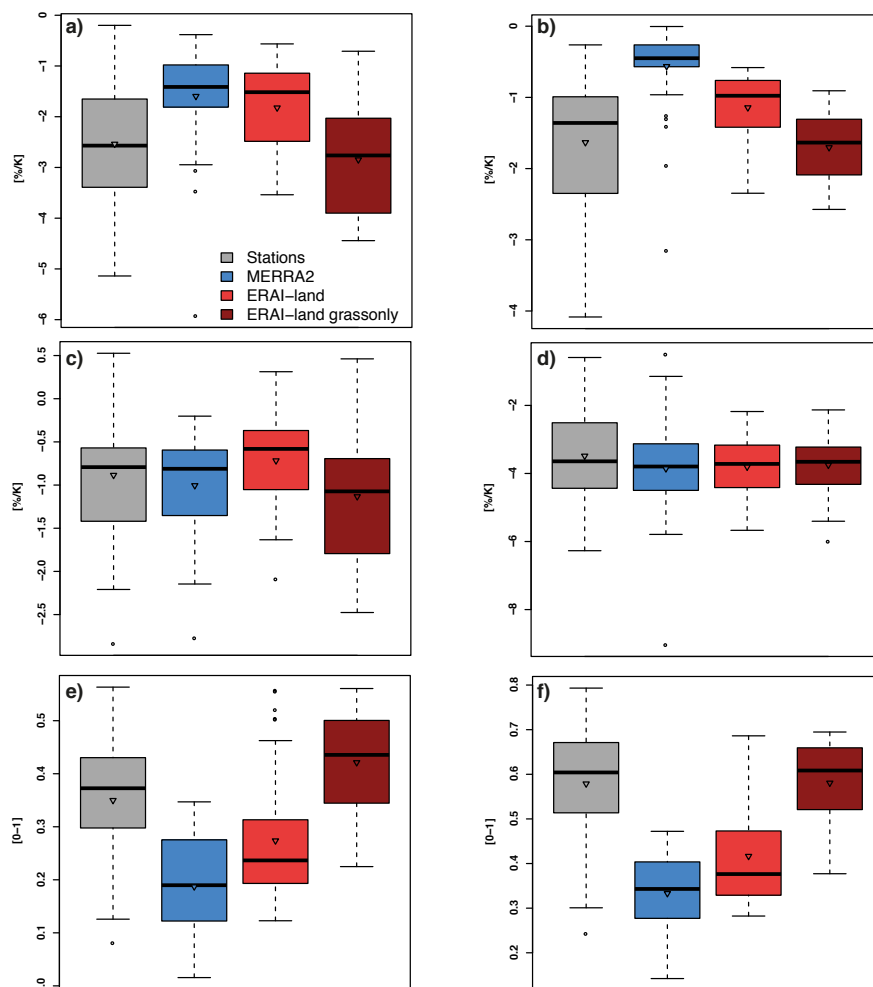


359 The further analysis of the two components of SAF (SNC and TEM, Figure 4 b and c)  
360 shows that ERAI-LG reproduces well the SNC signal derived from the station data (-  
361 1.6% K<sup>-1</sup> mean for stations and -1.7% K<sup>-1</sup> mean for ERAI-LG), whereas the other two  
362 reanalyses show much weaker SNC values. The lowest value of -0.56% K<sup>-1</sup> was  
363 obtained from the MERRA2 data. In general, SNC responses largely explain  
364 differences in SAF (Figure 4a).

365 For TEM values (Figure 4c), all three reanalyses are in a good agreement with the  
366 observations with MERRA2 showing the best agreement. Changing the vegetation to  
367 grass in ERA-Interim results in a TEM component, which is 0.4-0.5% K<sup>-1</sup> stronger  
368 compared to the standard version of ERA-Interim. Given that TEM represents the  
369 response to snow metamorphosis, good performance of MERRA2 is in agreement  
370 with findings implied by Figure 2. However it is worth noting that for the station  
371 network as well as for the ECMWF experiments, locations with positive TEM are  
372 calculated. This is due to snow albedo changes being positive in some instances  
373 (Figure 4c).

374 To further investigate the nature of the SNC and TEM responses we show in Figure  
375 4d the results for snow melt sensitivity, which is one of the two key components in  
376 the SNC response (1). This component is barely influenced by the underlying  
377 vegetation. All three reanalysis datasets agree very well with the station network, with  
378 ERAI-LG showing the closest agreement for both mean and median. This indicates an  
379 accurate representation of this relationship in both NASA and ECMWF land surface  
380 modules.

381 Figure 4d implies that the changes in the SNC should stem from the albedo contrast,  
382 the second key component expressed as the average difference between albedo values  
383 for a complete snowcover and snow-free conditions (Figure 4e). Indeed, MERRA2  
384 shows the lowest albedo contrast among all datasets, resulting in very low SNC  
385 values. Albedo contrast in ERAI-L is higher than MERRA2, but is on average still  
386 lower compared to the observations, which show average values around 0.35. ERAI-  
387 LG shows the strongest albedo contrast, which is twice as large compared to the  
388 experiment with classic vegetation cover. These striking differences among the  
389 datasets mainly drive the SNC results.



390

391 **Figure 4: Boxplot analysis for MAMJ 2000–2013 a) SAF, b) SNC, c) TEM, d) snow melt sensitivity, e)**  
 392 **albedo contrast and f) snow albedo. Triangle indicates the mean value.**

393

394 Snow albedo is well captured by the grass-only experiment showing the same average  
 395 value around 0.6 as determined from the observations (Figure 4f). The standard  
 396 vegetation schemes used in MERRA2 and ERAI-L reduce the snow albedo in the  
 397 analyzed grid cells to 0.33 and 0.37. The differences in snow albedo between the  
 398 products is the main driver for the differences in the albedo contrast since the snow-  
 399 free albedo values are remarkably similar for all reanalysis products (Figure 5a).  
 400 Nevertheless, they strongly deviate from the snow-free albedo determined from the  
 401 observations, which is roughly twice as large compared to the reanalyses with a mean





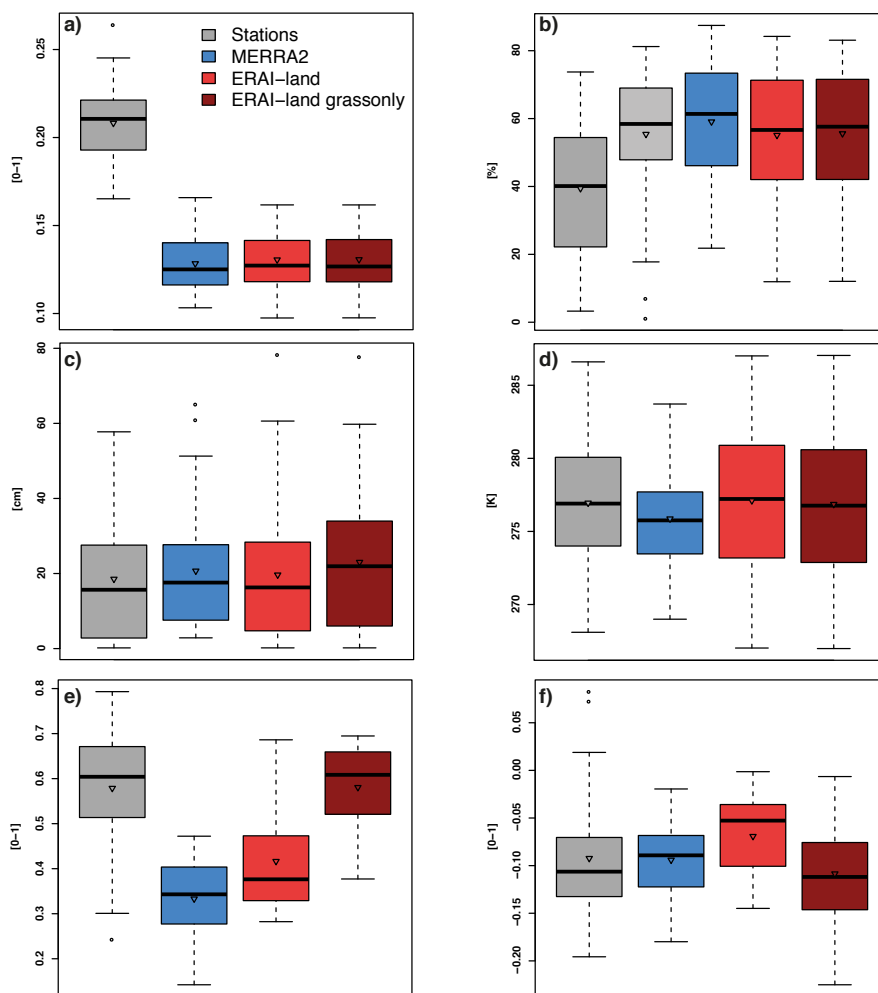
402 value of about 0.21 and which is very close to albedo values for grass (see e.g. **Betts**  
403 **and Ball 1997, Wei et al. 2001**).

404 To explore the impact of different factors on the TEM estimates, we show in Figure 5  
405 mean values of temperature, snow cover and albedo, as well as the average change of  
406 snow albedo during spring. Also, to underline the crucial role of in-situ snow depth  
407 information, mean snow depth is shown. Mean station snow depth lies within the  
408 range of reanalyses values, with higher values reported by ERAI-LG. Moreover,  
409 stations have the lowest snow cover among all datasets (Figure 5 b and c). This  
410 difference is likely due to the conversion of snow depth to snow cover as well as from  
411 the precision (in centimeters) of the Russian snow depth measurement. Precision of  
412 snow depth diagnosed by reanalysis is much finer and the logarithmic conversion here  
413 can be performed more accurately. As a result, TEM values diagnosed by stations are  
414 probably too low. If we consider instead in-situ snow cover information from stations,  
415 the average snow cover is quite similar to reanalyses (ca. 55%), and the average TEM  
416 value gets stronger. However, replacing converted snow cover with observed snow  
417 cover in Eq. (2) is a questionable procedure, as the remaining terms were computed  
418 using snow depth conversion. Thus, for consistency we show lower values of TEM in  
419 Figure 4.

420 Temperature is well represented by all datasets with MERRA2 being about 1 K colder  
421 compared to stations, which is quite notable for such a robust variable. However,  
422 absolute values of temperature do not have a strong impact on the computation of  
423 TEM, since month-to-month changes in temperature affect both TEM and SNC  
424 computations. For ERAI-LG, the effect of the underestimated snow-free albedo and  
425 overestimated complete snow cover albedo cancel each other out. Finally, the snow  
426 albedo change during spring season (Figure 5f) is very similar in station data and in  
427 MERRA2 (-0.09 average in both datasets), which points towards an adequate  
428 representation of snow metamorphosis and aerosol deposition in MERRA2. The  
429 ERAI-LG experiment shows a stronger change of snow albedo during spring than the  
430 standard version. ERAI-L potentially keeps the temperature and therefore snow  
431 metamorphosis more constant throughout spring season due to a more stable local  
432 temperature climate induced by the vegetation. Note also, that some stations show an  
433 increase of snow albedo during spring. This can be caused by fresh snow  
434 accumulation in late spring in some locations.



435  
 436  
 437



438

439 **Figure 5: Boxplot analysis for MAMJ 2000–2013 a) snow free albedo, b) snow cover fraction, where**  
 440 **the light grey boxplot is the originally observed snow cover from stations, c) snow depth, d) 2m**  
 441 **temperature, e) mean albedo and f) snow albedo change within the season. Triangle indicates the**  
 442 **mean value.**

443

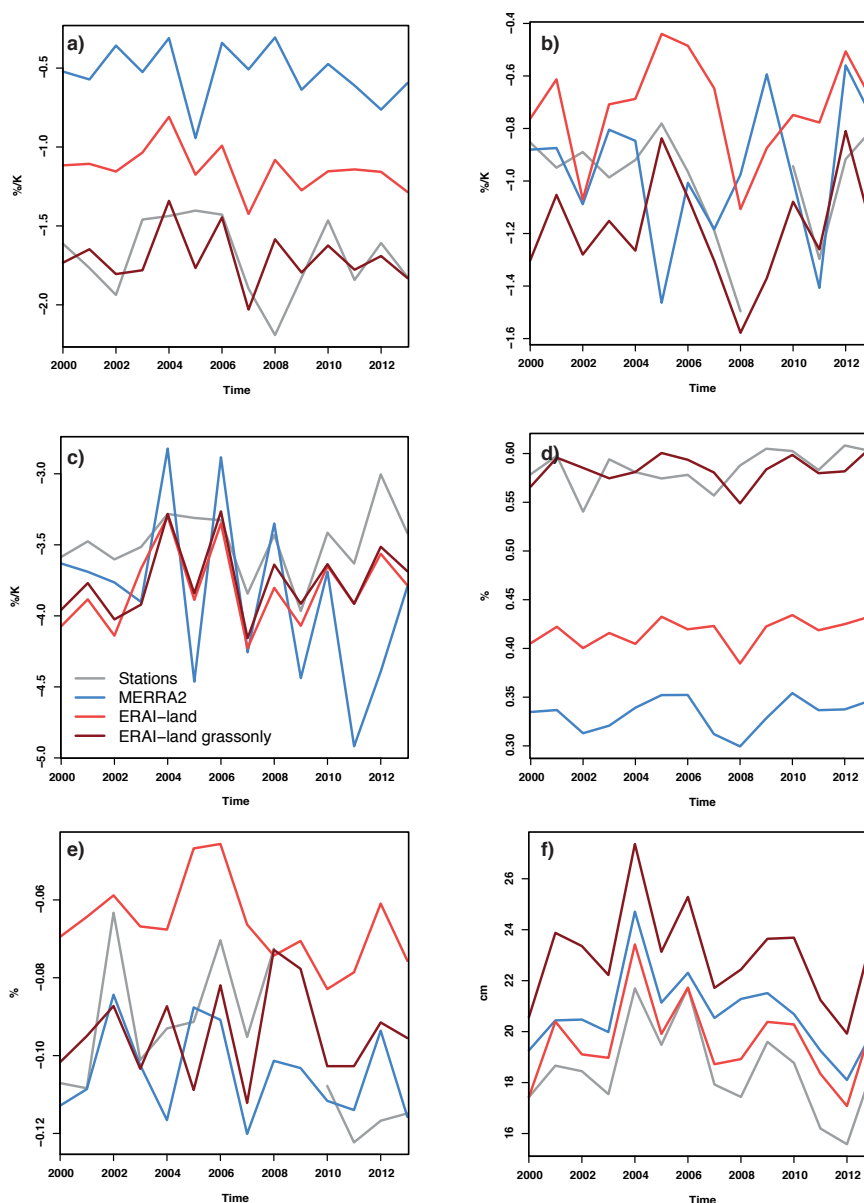
444 Figure 6 shows timeseries (2000–2013) for the mean values for SAF-related variables.  
 445 Timeseries for SNC (Figure 6a) and TEM (Figure 6b) show that inter-annual



446 variations of up to  $0.5\% \text{ K}^{-1}$  are possible for both stations and reanalyses. Moreover,  
447 for both SNC and TEM, ERAI-LG seems to reproduce well the overall baseline and  
448 the magnitude of variability.

449 For snow melt sensitivity (Figure 6c) the agreement among the datasets is very good  
450 for both magnitude and interannual variability, with MERRA2 showing an amplified  
451 inter-annual variability (up to  $1.5\% \text{ K}^{-1}$ ), which is beyond the magnitudes observed at  
452 stations. As already noted above, snow melt sensitivity seems to be a rather well  
453 reproduced process in modern reanalyses. Since snow-free albedo is quite constant  
454 over time in the reanalyses, the albedo contrast is dominated by the snow albedo  
455 (Figure 6d). ERAI-LG and the station network agree very well on the magnitude of  
456 snow albedo, whereas ERAI-L and MERRA2 fail to reproduce such high values.  
457 Magnitudes of inter-annual variability can reach up to  $\pm 0.05$  in stations, with slightly  
458 weaker response in reanalyses. Correlation between stations and reanalyses is rather  
459 low, only individual years are captured correctly by ERAI-LG (see Supplement for  
460 correlation values).

461 Snow albedo change within spring season (Figure 6e) is well captured by MERRA2  
462 and ERAI-LG. Furthermore, ERAI-LG captures well the inter-annual variability for  
463 this metric. Specifically, variability during 2001–2004 and 2005–2008 periods is quite  
464 well represented. On the other hand, ERAI-L seems to lack the consistency with  
465 observations. Finally, as it was mentioned in section 4.1, snow depth variability  
466 (Figure 6f) is very well captured by all reanalyses. Again, ERAI-LG overestimates  
467 snow depth by up to 5 cm, with the other two reanalyses being on average 1-2 cm  
468 above the station values.



469

470 **Figure 6: Yearly timeseries of selected MAMJ SAF components averaged over all 44 locations. a) SNC,**  
 471 **TEM, c) snow melt sensitivity, d) snow albedo, e) snow albedo change within the season, f) snow**  
 472 **depth.**

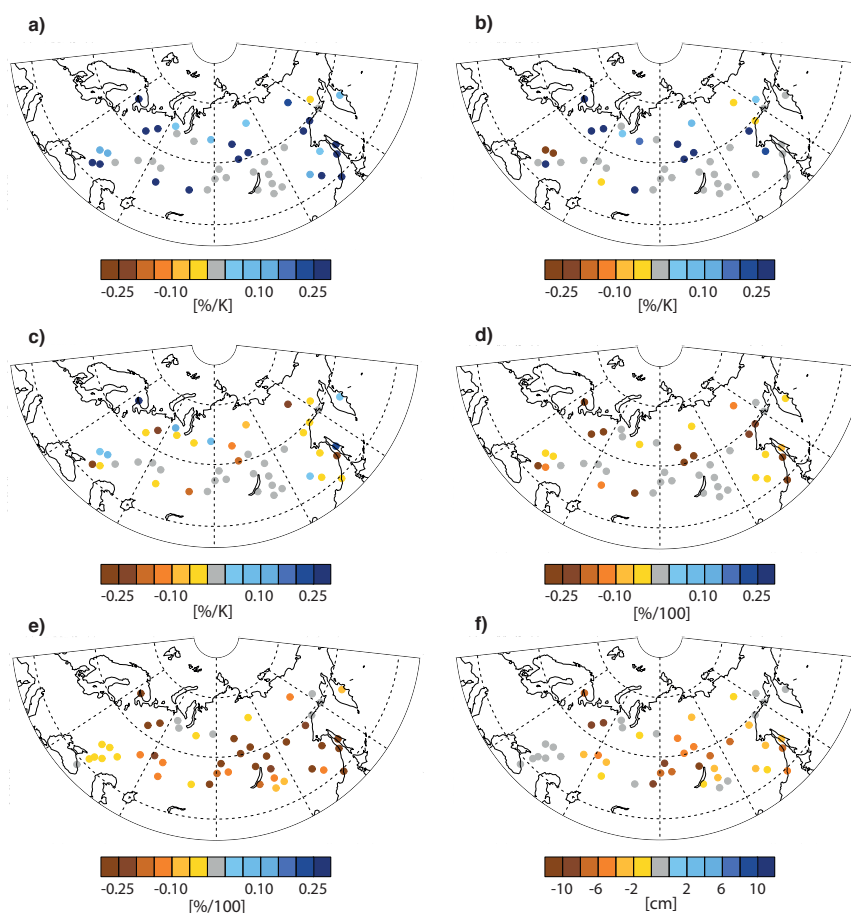
473

474 To further demonstrate the effect of the vegetation changes in the ERA-Interim land  
 475 reanalysis, Figure 7 shows anomalies between ERAI-L and ERAI-LG. The structure



476 follows Figure 6, with SNC and TEM shown in Figure 7a&b. As is clearly visible  
477 both variables are generally less negative in ERAI-L, a fact already known from  
478 timeseries and boxplot analysis. The largest impact of the vegetation changes is found  
479 for Northern Russia, the Pacific coast and the western region between Black and  
480 Caspian Sea. Interestingly, but as expected, snow melt sensitivity (Figure 6c) is not  
481 the key driver behind this distribution. Since snow melt sensitivity is not directly  
482 linked to vegetation changes, the anomaly distribution is very heterogenous, with  
483 positive and negative anomalies over the whole domain. As known from the  
484 timeseries plot, snow sensitivity in ERAI-LG is overall slightly weaker than in ERAI-  
485 L, probably due to positive feedbacks such as reduction of nighttime cooling over  
486 higher vegetation types. The main driver behind the distribution of SNC is albedo  
487 contrast (Figure 7d). Albedo contrast is overall higher in ERAI-LG, especially along  
488 the borders of the domain, highlighted already for SNC.

489



490

491 **Figure 7: Mean SAF components in anomalies of ERAI-L minus ERAI-LG for 2000-2013 MAMJ. a) SNC,**  
492 **b) TEM, c) snow melt sensitivity, d) mean albedo contrast, e) mean albedo, f) snow depth.**

493

## 494 5. Discussion

495 We compared spring SAF and its components determined from in-situ measurements  
496 over Russia for the period 2000–2013 with data derived from three modern reanalysis  
497 products restricted to the grid cells including the observational sites. This was  
498 achieved by using a unique collection of station measurements of radiation and snow  
499 characteristics investigating for the first time observed SAF over this broad spatial  
500 and temporal domain. Besides ERAI-L we also used a customized version of ERAI-L  
501 (ERAI-LG), in which vegetation was set to grass in all concerned grid cells. All three  
502 reanalysis datasets are completely independent from the analyzed station data. While



503 a direct comparison of point measurements with grid cell output always introduces  
504 uncertainties properties due to the spatial variability of the surface, this is for now the  
505 only way to evaluate reanalyses data using in-situ observations. An alternative option  
506 would be the satellite data, which come with their own uncertainties (e.g. **Romanov**  
507 **et al. 2002, Foster et al. 2005, Wang et al. 2014**).

508 Snow depth statistics derived from daily station data are reasonably well reproduced  
509 in all three modern reanalyses, which is in agreement with **Wegmann et al. (2017)**  
510 who investigated April snow depth in ERAI-L. While snow depth differences  
511 between ERAI-L and ERAI-LG are small, ERAI-LG shows slightly higher deviations  
512 from the station data than ERAI-L that might be caused by the higher vegetation in  
513 station surroundings and by underestimation of snowfall due to instrumentation used  
514 at the Russian station network (**Rasmussen et al. 2012**).

515 Day-to-day variability of albedo is notably higher in station data compared to any  
516 reanalysis product. Besides spatial averaging over the reanalyses grid cells, this is  
517 potentially caused by land surface changes due to weather (e.g. vegetation changes,  
518 flooding, frost, aerosol deposition), which are not represented in the reanalyses.  
519 However, ERAI-LG demonstrates increasing albedo variability, nearly doubling the  
520 standard deviations diagnosed by ERAI-L with the standard vegetation scheme.

521 The limitations of the station data imply some constraints for comparisons with  
522 reanalysed data. As near-surface temperature is unavailable in station data, we used  
523 for both stations and reanalyses 2m air temperature, which reduces the strength of the  
524 SAF feedback. Secondly, snow cover is underestimated in station data due to the  
525 measurement precision of 1cm, which reduces the strength of the TEM component.  
526 The snow albedo and the snow-free albedo are substantially higher in station data than  
527 in the reanalyses with classic vegetation boundary conditions (MERRA2 and ERAI-  
528 L). Compared to other observation-based studies, spring snow albedo and grass  
529 albedo derived from our station network is quite realistic (**Roesch et al. 2009,**  
530 **Stroeve et al. 2006**). Thus, the difference revealed by reanalyses is likely due to  
531 averaging over grid cells.

532 Results from ERAI-LG clearly demonstrate that SAF and its components are very  
533 close to those in the station data. The largest improvement was found for albedo  
534 contrast and for snow albedo, which both are more realistic in ERAI-LG. At the same



535 time snow-free albedo in all three reanalyses (including ERAI-LG) was found to be  
536 lower than in the station data because snow-free albedo in all reanalysis data sets is  
537 prescribed as a monthly climatology from MODIS data.

538 MERRA2 shows the lowest SAF values resulting from a very low albedo contrast,  
539 which is probably a consequence of the vegetation scheme in the MERRA2 land  
540 module. On the other hand, MERRA2 represents TEM reasonably well most likely  
541 due to the accurate representation of the intra-seasonal snow albedo changes. Thus,  
542 relative snowpack changes appear to be well represented in MERRA2, probably also  
543 due to a more accurate representation of aerosols.

544 In general, we found higher SAF values in ERAI-L than in the recent CMIP3/5  
545 analyses of NH SAF by **Fletcher et al. (2015)**. This disagreement results from a  
546 variety of factors. First, our domain is limited to Russia only, thus excluding  
547 considerable parts of Eurasia as well as North America. In this respect our domain is  
548 set within a high SAF region, which may explain higher SAF values compared to the  
549 NH average by **Fletcher et al. (2015)**. On the other hand, MERRA2 shows good  
550 agreements with the NH CMIP4/5 SAF results, however mostly because the albedo  
551 contrast is very low. Furthermore, as we pointed out above, in-situ observations used  
552 here tend to slightly overestimate SAF, mainly due to higher snow albedo values. This  
553 is because in-situ snow albedo is typically measured by a sensor installed over a  
554 vegetation-free snow pack. The vegetation scheme used in reanalyses gives lower  
555 snow albedo values implying realistic vegetation cover such as taiga or tundra.  
556 However, our MERRA2 results agree fairly well with the findings of **Fletcher et al.**  
557 **(2015)**. Moreover, mean values of the albedo independent variable snow melt  
558 sensitivity are very close to the "observational" snow melt sensitivity computed by  
559 **Fletcher et al. (2015)**.

560 We also found agreements with **Fletcher et al. (2015)** in the representation of the  
561 spatial pattern of the SAF components. **Fletcher et al. (2015)** as well as **Fernandes et**  
562 **al. (2009)** have shown maxima in SAF over northern Canada, northern Siberia and  
563 southwestern Eurasia. The relation of 60:40 found in satellites and reanalysis for SNC  
564 to TEM was replicated by our station network. We found similar spatial patterns for  
565 SAF and its components in both stations and gridded data specifically for Southern  
566 Russia, while the pattern of station responses is less homogenous compared to the





567 gridded data. Also consistent with **Fletcher et al. (2015)**, we found higher snow melt  
568 sensitivity north of 50° N. Finally, albedo contrast distribution, which closely follows  
569 the snow albedo pattern, is in very good agreement with the gridded analysis of snow  
570 albedo by **Fletcher et al. (2015)**.

## 571 **6. Conclusions**

572 Reanalyses including land surface modules show a physically consistent  
573 representation of SAF with realistic spatial patterns and area-averaged sensitivity  
574 estimates. ERAI-LG shows a better performance in representing station-based  
575 estimates considering the uncertainty associated with "point to grid cell" comparisons.  
576 Accounting for aerosol-related processes would likely improve this performance in  
577 future reanalysis releases. Thus, for the analysis and validation of large-scale temporal  
578 and spatial averages of SAF modern reanalyses seem to be an appropriate tool.

579 However, for analysing processes on smaller scales and high temporal resolution  
580 studies, a healthy dense station network is required. The idealized ERAI-LG  
581 simulation also highlights the caveats of comparing in-situ observations with gridded  
582 model data. In this study, we show these discrepancies in terms of albedo and snow  
583 depth. Other variables, in particular 2m temperature, can be expected to have a similar  
584 signal arising from the differences between the model's gridcell land cover and the  
585 actual station conditions. Our findings show that the experimental approach in ERAI-  
586 LG allows for an enhanced use of in-situ observations to diagnose the SAF in not-  
587 forested areas.

588 Considering future studies, the extension to other regions and use of other regional in-  
589 situ data might give further insights into regional hotspots of SAF. Cross-validation  
590 efforts employing model, reanalysis, satellite and station data may help to generate  
591 blended products to investigate radiation and albedo feedbacks in the changing Arctic,  
592 a region where SAF is especially strong. Regional modelling, including a variety of  
593 multi-layer land surface models over areas with a relatively dense observation  
594 network can provide a quantitative estimation of uncertainties among complex  
595 variables such as snow depth, albedo or SAF.

596



597 *Acknowledgements.* This study was supported by the ARCTIC-ERA project funded by  
598 the Belmont Forum Fund through the ANR. OZ also benefited from the support by  
599 the Russian Ministry of Education and Science (project no. 14.B25.31.0026). ED was  
600 supported by FCT (IF/00817/2015).  
601

602



603 **References**

- 604 Balsamo, G., Albergel, C., Beljaars, A., Boussetta, S., Brun, E., Cloke, H., Dee, D.,  
605 Dutra, E., Muñoz-Sabater, J., Pappenberger, F., de Rosnay, P., Stockdale, T. &  
606 Vitart, F. 2015: ERA-Interim/Land: a global land surface reanalysis data set.  
607 Hydrology and Earth System Sciences, 19, 389-407
- 608 Betts, A. K., & Ball, J. H. 1997: Albedo over the boreal forest. Journal of Geophysical  
609 Research: Atmospheres, 102, 28901-28909.
- 610 Bony, S., Colman, R., Kattsov, V.M., Allan, R.P., Bretherton, C.S., Dufresne, J., Hall,  
611 A., Hallegatte, S., Holland, M.M., Ingram, W., Randall, D.A., Soden, B.J.,  
612 Tselioudis, G. and Webb M.J. 2006: How Well Do We Understand and Evaluate  
613 Climate Change Feedback Processes?. J. Climate, 19, 3445–3482
- 614 Brun, E., Vionnet, V., Boone, A., Decharme, B., Peings, Y., Valette, R., Karbou, F.,  
615 and Morin, S 2013: Simulation of Northern Eurasian Local Snow Depth, Mass,  
616 and Density Using a Detailed Snowpack Model and Meteorological Reanalyses, J.  
617 Hydrometeorol., 14, 203–219
- 618 Brutel-Vuilmet, C., Ménégoz, M., & Krinner, G. 2013: An analysis of present and  
619 future seasonal Northern Hemisphere land snow cover simulated by CMIP5  
620 coupled climate models. The Cryosphere, 7, 67
- 621 Budkyo, M. I. 1967: The effect of solar radiation on the climate of the earth. Tellus,  
622 21, 611-19
- 623 Bulygina, O. N., Groisman, P. Y., Razuvaev, V. N., & Radionov, V. F. 2010: Snow  
624 cover basal ice layer changes over Northern Eurasia since 1966. Environmental  
625 Research Letters, 5, 015004.
- 626 Cess, R. O., & Potter, G. L. 1991: Interpretation of snow-climate feedback as  
627 produced by 17 general circulation models. Science, 253, 888
- 628 Cohen, J., Screen, J. A., Furtado, J. C., Barlow, M., Whittleston, D., Coumou, D.,  
629 Francis, J., Dethloff, K., Entekhabi, D. & Overland J. 2014: Recent Arctic  
630 amplification and extreme mid-latitude weather. Nat. Geosci., 7, 627–37



- 631 Collins, M., Knutti, R., Arblaster, J., Dufresne, J.-L., Fichefet, T., Friedlingstein, P.,  
632 Gao, X., Gutowski, W.J., Johns, T., Krinner, G., Shongwe, M., Tebaldi, C.,  
633 Weaver, A.J. & Wehner M. 2013: Long-term Climate Change: Projections,  
634 Commitments and Irreversibility. In: Climate Change 2013: The Physical Science  
635 Basis. Contribution of Working Group I to the Fifth Assessment Report of the  
636 Intergovernmental Panel on Climate Change [Stocker, T.F., D. Qin, G.-K. Plattner,  
637 M. Tignor, S.K. Allen, J. Boschung, A. Nauels, Y. Xia, V. Bex and P.M. Midgley  
638 (eds.)]. Cambridge University Press, Cambridge, United Kingdom and New York,  
639 NY, USA.
- 640 Curry, J. A., Schramm, J. L., Rossow, W. B., & Randall, D. 1996: Overview of Arctic  
641 cloud and radiation characteristics. *Journal of Climate*, 9, 1731-1764.
- 642 Dee, D. P., Uppala, S. M., Simmons, A. J., Berrisford, P., Poli, P., Kobayashi, S.,  
643 Andrae, U., Balmaseda, M. A., Balsamo, G., Bauer, P., Bechtold, P., Beljaars, A.  
644 C. M., van de Berg, L., Bidlot, J., Bormann, N., Delsol, C., Dragani, R., Fuentes,  
645 M., Geer, A. J., Haimberger, L., Healy, S. B., Hersbach, H., Hólm, E. V., Isaksen,  
646 L., Kållberg, P., Köhler, M., Matricardi, M., McNally, A. P., Monge-Sanz, B. M.,  
647 Morcrette, J.-J., Park, B.-K., Peubey, C., de Rosnay, P., Tavolato, C., Thépaut, J.-  
648 N., & Vitart, F. 2011: The ERA-interim reanalysis: Configuration and  
649 performance of the data assimilation system, *Q. J. Roy. Meteor. Soc.*, 137, 553–  
650 597
- 651 Derksen, C. & R. Brown, 2012: Spring snow cover extent reductions in the 2008–  
652 2012 period exceeding climate model projections. *Geophysical Research Letters*,  
653 39.
- 654 Dufour, A., Zolina, O. and Gulev, S.K., 2016: Atmospheric moisture transport to the  
655 Arctic: Assessment of reanalyses and analysis of transport components. *Journal of*  
656 *Climate*, 29, 5061-5081.
- 657 Dutra, E., Balsamo, G., Viterbo, P., Miranda, P. M., Beljaars, A., Schär, C., & Elder,  
658 K. 2010: An improved snow scheme for the ECMWF land surface model:  
659 description and offline validation. *Journal of Hydrometeorology*, 11, 899-916.
- 660 Fernandes, R., H. Zhao, X. Wang, J. Key, X. Qu, & A. Hall 2009: Controls on



- 661 Northern Hemisphere snow albedo feedback quantified using satellite earth  
662 observations, *Geophys. Res. Lett.*, 36, L21702
- 663 Flanner, M. G., Shell, K. M., Barlage, M., Perovich, D. K., & Tschudi, M. A. 2011:  
664 Radiative forcing and albedo feedback from the Northern Hemisphere cryosphere  
665 between 1979 and 2008. *Nature Geoscience*, 4, 151.
- 666 Fletcher, C. G., Thackeray, C. W., & Burgers, T. M. 2015 Evaluating biases in  
667 simulated snow albedo feedback in two generations of climate models. *Journal of*  
668 *Geophysical Research: Atmospheres*, 120, 12-26.
- 669 Fletcher, C. G., Zhao, H., Kushner, P. J., & Fernandes, R. 2012: Using models and  
670 satellite observations to evaluate the strength of snow albedo feedback. *Journal of*  
671 *Geophysical Research: Atmospheres*, 117
- 672 Foster, J. L., Sun, C., Walker, J. P., Kelly, R., Chang, A., Dong, J., & Powell, H.  
673 2005: Quantifying the uncertainty in passive microwave snow water equivalent  
674 observations. *Remote Sensing of environment*, 94, 187-203
- 675 Gelaro, R., McCarty, W., Suárez, M.J., Todling, R., Molod, A., Takacs, L., Randles,  
676 C.A., Darmenov, A., Bosilovich, M.G., Reichle, R., Wargan, K., Coy, L.,  
677 Cullather, R., Draper, C., Akella, S., Buchard, V., Conaty, A., da Silva, A.M., Gu,  
678 W., Kim, G., Koster, R., Lucchesi, R., Merkova, D., Nielsen, J.E., Partyka, G.,  
679 Pawson, S., Putman, W., Rienecker, M., Schubert, S.D., Sienkiewicz, M. & Zhao  
680 B. 2017: The Modern-Era Retrospective Analysis for Research and Applications,  
681 Version 2 (MERRA-2). *J. Climate*, 30, 5419–5454
- 682 Graverson, R. G., & Wang, M. 2009: Polar amplification in a coupled climate model  
683 with locked albedo. *Climate Dynamics*, 33, 629-643
- 684 Graverson, R. G., Langen, P. L., & Mauritsen, T. 2014: Polar amplification in  
685 CCSM4: Contributions from the lapse rate and surface albedo feedbacks. *Journal*  
686 *of Climate*, 27, 4433-4450.
- 687 Groisman, P. Y., Karl, T. R., Knight, R. W., & Stenchikov, G. L. 1994: Changes of  
688 snow cover, temperature, and radiative heat balance over the Northern  
689 Hemisphere. *Journal of Climate*, 7, 1633-1656.



- 690 Hall, A. 2004: The role of surface albedo feedback in climate. *Journal of Climate*, 17,  
691 1550-1568.
- 692 Hall, A., & Qu, X. 2006: Using the current seasonal cycle to constrain snow albedo  
693 feedback in future climate change. *Geophysical Research Letters*, 33(3).
- 694 Hall, A., Qu, X., & Neelin, J. D. 2008 Improving predictions of summer climate  
695 change in the United States. *Geophysical Research Letters*, 35
- 696 Hirahara, S., Ishii, M., & Fukuda, Y. 2014: Centennial-scale sea surface temperature  
697 analysis and its uncertainty. *Journal of Climate*, 27, 57-75.
- 698 Kanamitsu, M., Ebisuzaki, W., Woollen, J., Yang, S. K., Hnilo, J. J., Fiorino, M., &  
699 Potter, G. L. 2002: Ncep–doe amip-ii reanalysis (r-2). *Bulletin of the American*  
700 *Meteorological Society*, 83, 1631-1643.
- 701 Kobayashi, S., Yukinari, O.T.A., Harada, Y., Ebita, A., Moriya, M., Onoda, H.,  
702 Onogi, K., Kamahori, H., Kobayashi, C., Miyaoka, K. & Takahashi, K., 2015: The  
703 JRA-55 reanalysis: General specifications and basic characteristics. *Journal of the*  
704 *Meteorological Society of Japan*. Ser. II, 93, 5-48.
- 705 Lian, M. S., & Cess, R. D. 1977: Energy balance climate models: A reappraisal of  
706 ice-albedo feedback. *Journal of the Atmospheric Sciences*, 34, 1058-1062.
- 707 Lindsay, R., Wensnahan, M., Schweiger, A., & Zhang, J. 2014: Evaluation of seven  
708 different atmospheric reanalysis products in the Arctic. *Journal of Climate*, 27,  
709 2588-2606.
- 710 Molod, A., Takacs, L., Suarez, M., & Bacmeister, J. 2015: Development of the  
711 GEOS-5 atmospheric general circulation model: evolution from MERRA to  
712 MERRA2. *Geoscientific Model Development*, 8, 1339-1356.
- 713 Qu, X., & Hall, A. 2007: What controls the strength of snow-albedo feedback?.  
714 *Journal of Climate*, 20, 3971-3981.
- 715 Qu, X., & Hall, A. 2014: On the persistent spread in snow-albedo feedback. *Climate*  
716 *dynamics*, 42, 69-81



- 717 Rasmussen, R., Baker, B., Kochendorfer, J., Meyers, T., Landolt, S., Fischer, A.P.,  
718 Black, J., Thériault, J.M., Kucera, P., Gochis, D., Smith, C., Nitu, R., Hall, M.,  
719 Ikeda, K., & Gutmann E. 2012: How Well Are We Measuring Snow: The  
720 NOAA/FAA/NCAR Winter Precipitation Test Bed. *Bull. Amer. Meteor. Soc.*, 93,  
721 811–829
- 722 Reichle, R. H., Draper, C. S., Liu, Q., Giroto, M., Mahanama, S. P., Koster, R. D., &  
723 De Lannoy, G. J. 2017: Assessment of MERRA-2 land surface hydrology  
724 estimates. *Journal of Climate*, 30, 2937-2960.
- 725 Rienecker, M.M., Suarez, M.J., Gelaro, R., Todling, R., Bacmeister, J., Liu, E.,  
726 Bosilovich, M.G., Schubert, S.D., Takacs, L., Kim, G., Bloom, S., Chen, J.,  
727 Collins, D., Conaty, A., da Silva, A., Gu, W., Joiner, J., Koster, R.D., Lucchesi, R.,  
728 Molod, A., Owens, T., Pawson, S., Pegion, P., Redder, C.R., Reichle, R.,  
729 Robertson, F.R., Ruddick, A.G., Sienkiewicz, M. & Woollen, J. 2011: MERRA:  
730 NASA's Modern-Era Retrospective Analysis for Research and Applications. *J.*  
731 *Climate*, 24, 3624–3648  
732
- 733 Robock, A. 1983: Ice and snow feedbacks and the latitudinal and seasonal distribution  
734 of climate sensitivity. *Journal of the Atmospheric Sciences*, 40, 986-997.
- 735 Roesch, A., Gilgen, H., Wild, M., & Ohmura, A. 1999: Assessment of GCM  
736 simulated snow albedo using direct observations. *Climate dynamics*, 15, 405-418.
- 737 Romanov, P., Gutman, G., & Csiszar, I. 2002: Satellite-derived snow cover maps for  
738 North America: accuracy assessment. *Advances in space Research*, 30, 2455-2460.
- 739 Schiffer, R. A., & Rossow, W. B. 1983 The International Satellite Cloud Climatology  
740 Project (ISCCP)- The first project of the World Climate Research Programme.  
741 *American Meteorological Society, Bulletin*, 64, 779-784.
- 742 Schneider, S. H., & Dickinson, R. E. 1974: Climate modeling. *Reviews of*  
743 *Geophysics*, 12, 447-493.
- 744 Serreze, M. C., & Barry, R. G. 2011: Processes and impacts of Arctic amplification:  
745 A research synthesis. *Global and Planetary Change*, 77, 85-96.



- 746 Stroeve, J. C., Box, J. E., & Haran, T. 2006: Evaluation of the MODIS (MOD10A1)  
747 daily snow albedo product over the Greenland ice sheet. *Remote Sensing of*  
748 *Environment*, 105, 155-171.
- 749 Thackeray, C. W., & Fletcher, C. G. 2016: Snow albedo feedback: Current  
750 knowledge, importance, outstanding issues and future directions. *Progress in*  
751 *Physical Geography*, 40, 392-408.
- 752 Wang, Z., Schaaf, C.B., Strahler, A.H., Chopping, M.J., Román, M.O., Shuai, Y.,  
753 Woodcock, C.E., Hollinger, D.Y. & Fitzjarrald, D.R. 2014: Evaluation of MODIS  
754 albedo product (MCD43A) over grassland, agriculture and forest surface types  
755 during dormant and snow-covered periods. *Remote Sensing of Environment*, 140,  
756 60-77.
- 757 Wei, X., Hahmann, A. N., Dickinson, R. E., Yang, Z. L., Zeng, X., Schaudt, K. J.,  
758 Schaaf, C.B. & Strugnell, N. 2001: Comparison of albedos computed by land  
759 surface models and evaluation against remotely sensed data. *Journal of*  
760 *Geophysical Research: Atmospheres*, 106, 20687-20702.
- 761 Wegmann, M., Orsolini, Y., Dutra, E., Bulygina, O., Sterin, A., & Brönnimann, S.  
762 2017: Eurasian snow depth in long-term climate reanalyses. *The Cryosphere*, 11,  
763 923.
- 764 Wexler, H. 1953: Radiation balance of the Earth as a factor in climatic change. In:  
765 Shapley H (ed) *Climatic Change*. Cambridge: Harvard University Press,73-105